ISSN 1330-3651 (Print), ISSN 1848-6339 (Online)
Received: 1 September 2025; Accepted: 21 October 2025

https://doi.org/10.17559/TV-20250901002935
Subject Review

Review of Fabrication Methods Employed for 3D Printing DSS Parts using GMAW-AM Process: A Systematic Analysis

Uhamir PATRICK*, Stefanija KLARIC, Sara HAVRLISAN*

Abstract: Research studies on the Duplex Stainless Steel (DSS) parts fabricated by the Gas Metal Arc Welding-Additive Manufacturing (GMAW-AM) process have revealed that undesired deposition geometry, ferrite-austenite (α-γ) phase imbalance, sigma (σ) phase formation, and anisotropic properties are a usual predicament, given the complex nature of the GMAW-AM process and highly sensitive alloy composition of the DSS. To what extent these problems have been resolved is a pertinent question. This study systematically reviewed the research published in the last ten years involving different GMAW-AM methods for DSS parts fabrication. Particularly, the translated effects of process parameter optimisation, shielding gas combination, and special material and mechanism assisted methods on the geometrical, microstructural and performance characteristics of parts were critically analysed. The results showed that the research intervention for enhancing metallographic and mechanical attributes of GMAW-AM-based DSS parts has a high merit for obtaining tailored grain growth, crystal formation, and balanced α-γ phases with minimal σ phases. A suitable fabrication route, backed by available literature, is presented to provide future research directions.

Keywords: DSS parts; fabrication methods; GMAW-AM; mechanical performance; microstructural characteristics; systematic review

1 INTRODUCTION

Research interest in the fabrication of DSS parts by the GMAW-AM process has grown impressively, especially over the last decade. Backed by equal proportions of α-γ phases, DSS parts are extensively employed by chemical processing, petro-gas, pulp making, power generation, and marine industries due to their strength and exceptional corrosion resistance [1]. Among various MAM processes, the GMAW-AM uniquely employs filler wire fed into a welding robot to deposit successive layers using arc energy as per the geometric requirements [2]. The layer-by-layer production method enables the deposited material to solidify quickly, unlike the traditional casting methods. This has enabled the development of unique and complex geometries in a much faster production time [3].

However, the inherent heating and cooling cycles of the process often complicate the geometrical, microstructural, and mechanical characteristics of fabricated parts. Having a rich and thermally sensitive alloy composition, fabrication of DSS parts with suitable properties using the GMAW-AM process remains a research challenge. Prominent geometric imperfections include waviness and lumpiness in deposited layers, inconsistent bead geometry, and non-alignment of successive beads due to lateral movements. From the microstructure perspective, grain coarsening, boundary area reduction, α-γ phase imbalance and σ phase formation, degrade parts performance and commercial prospects [4, 5]. Available studies highlight that both the cause and cure of incompetencies in fabricated parts lie in the fabrication method.

Review of the body of research suggests that optimisation of welding parameters could overcome geometrical defects and ensure dimensional integrity in deposited layers. It is also observed that parametric optimisation could be combined with specialised gas mixtures and novel mechanisms to promote desired α and γ phase formations, reshape deposited geometry, and tailor alloy composition to a particular requirement. To chart out a commercially viable fabrication route, it is necessary to review each method and map its translated effects on parts geometric morphology, microstructural developments, and mechanical behaviour.

Therefore, the aim of this study is to review fabrication methods employed to develop DSS parts using GMAW-AM process. It endeavours to provide a comprehensive understanding of the translated effects of different fabrication mechanisms on the deposition geometry, phases formed, grain and boundary characteristics, and the resulting hardness, toughness, ductility, and tensile properties. The novelty of the study lies in its approach and the broad spectrum of research data that has been analysed (2015 to 2025). This study is unique as it objectively identifies the existing knowledge gaps and addresses them with concrete future recommendations.

2 METHODICAL FRAMEWORK

Successfully achieving the targeted outcomes from a research study requires a solid methodical foundation. Therefore, from the identification of databases to the selection of data for analysis, this study employed a methodical framework, shown in Tab. 1.

Table 1 Methodical framework for data collection and analysis

	Methodical Framework
Database	Following 'research' databases were searched: 1. American Society of Materials International (1) 2. American Society of Mechanical Engineers (0) 3. American Society of Testing and Materials (1) 5. Charles Darwin University (1) 6. Crainfield University (1) 7. Croatian Research Information System (CroRIS) (2) 8. Elsevier-Science Direct (21) 9. IEEE Xplore (0) 10. International Institute of Welding (4) 11. Institute of Materials, Minerals and Mining (1) 12. John Wiley and Sons Limited (1) 13. Korean Institute of Metals and Materials (3) 14. Multidisciplinary Digital Publishing Institute (10) 15. Paradigm Reference-Global (Sciendo) (1) 16. SAE International (1) 17. Sage (1) 18. Springer-Nature (18) 19. Taylor & Francis Group (0) 20. University of Slavonski Brod (1)

Table 1 Methodical framework for data collection and analysis - continuation

	Methodical Framework
	21. Miscellaneous (3) Following 'conference' databases were searched: 1. Danube Adria Association for Automation & Manufacturing (DAAAM) Conference (1) 2.MATEC Web of Conference (1) 3.13th International Scientific-Professional Conference SBW, 2025 (1) Following 'theses' databases were searched: 1. Cambridge.org (1) 2. ProQuest (1)
Keywords	3D printed DSS (0) AM of DSS (37) DED-arc of DSS (1) GMAW-AM of DSS (3) MAM of DSS (1) MIG-AM of DSS (1) WAAM of DSS (30)
Timeframe	March 2024 to August 2025
Inclusion Criteria (61 studies qualified)	1. Original research involving DSS alloys and the GMAW-AM process. 2. Research published as journal article, conference paper, or thesis. 3. Studies reporting experimental and standardised testing results. 4. Cited, at least once. 5. Indexed in Google Scholar, Scopus, Web of Science, or at least in one of the popular research platforms. 6. Open-access.
Exclusion Criteria (5 studies qualified)	1. Review Paper. 2. Non-cited.
Outcome	61 research studies were systematically selected for the review of DSS parts fabricated using the GMAW-AM process.

3 REVIEW AND ANALYSIS

3.1 Process Parameter Optimisation-Based Fabrication

The optimisation of the GMAW-AM process for the fabrication of DSS parts with suitable microstructure and appreciable properties remains as relevant as ever. The available literature indicates that parametric optimisation is the preferred route for researchers to produce DSS parts with adequate characteristics. Systematic methods for parametric optimisation include the application of DOE, OFAT, BOP, and MPO to rationalize the supplied DE [14, 19, 61, 62]. This section aims to review the effect of parametric optimization and the resulting DE on parts geometry, α-γ phases, σ phase, and mechanical properties. Some studies also employed post-process heat treatments to optimise grain structure and restore the α-γ phase balance. Since post-process treatments were not within the scope of this study, they were not considered for analysis.

3.1.1 Geometrical Appearance

For the sustainability of the fabrication process, it is essential that the deposited parts have high density, less filler material consumption, and least post-process machining requirements. The dimensional integrity of fabricated parts should be acceptable in terms of the deposition area, optimal width, and height of each deposited layer, with acceptable depth of penetration [6]. Optimum process parameters are vital to develop parts with improved bead morphology obtained with the minimum number of layers [7]. This reduces the overall production cost and time [8].

According to Knezović et al. [9], due to successive layer deposition, the deposited material continued to settle downwards, resulting in a decrease in overall height. They suggested that deposition of limited or few layers was not suitable for a reliable analysis [9]. In another study by Knezović et al. [10], different ILTs accounted for different geometrical appearances and properties of DSS parts fabricated using the GMAW-AM process. Three 3 ILTs (50 °C, 100 °C, and 150 °C) were employed to analyse their effect on net process duration. The results indicated that productivity was maximum with the highest ILT. While porosities were observed in all samples, the one obtained with 50 °C ILT had the highest porosity [10].

Some studies involved SDSS, which contain higher percentages of α stabilisers (Cr, Mo) and γ stabilisers (Ni, N), giving them more improved mechanical and electrochemical properties than the standard DSS [11]. A study on GMAW-AM-based production of SDSS parts found that structures involving multiple layers had less geometrical stability at higher IPTs [12]. During GMAW-AM-based fabrication of SDSS parts, Kumar and Maji [13] found that the *WFS* and *V* had a direct relationship with the bead dimensions and production rate during the GMAW-AM of SDSS parts. The research indicated that a higher flow rate of shielding gas and *TS* influenced bead dimensions and production rate inversely due to less material deposition per unit length [13]. Recently, Kumar et al. [14] employed ML-based MPO for optimum SGFR, *V*, *TS*, and *WFS* for GMAW-AM process. The method improved the overall height of the deposited SDSS structure and deposition efficiency [14].

In some studies, CMT technology was employed for DSS parts manufacturing. CMT is the modified version of the GMAW-AM process in which the metal droplets are deposited in a point-by-point or spot-by-spot manner during the layer deposition. As the DE input is significantly reduced, this technique is instrumental in controlling the thermal gradients and overall temperatures achieved during the process [15]. Nikam et al. [16] performed surface characterisation of fabricated parts. Their results indicated that CMT-based parts were comparable to hot-rolled cast DSS in terms of surface quality [16]. They suggested that CMT improved arc stability, which mitigated the risk of porosities and spatter formation [16]. According to Pant et al. [17], the CMT improved the geometrical consistency of deposited beads. The fabricated parts were devoid of macroscopic or visual defects due to increased process efficiency possible with CMT [17]. In the research by Hosseini et al. [18] two types of walls structures were fabricated using a higher ILT of 250 °C and a lower ILT of 150 °C. However, production time with each ILT was different due to the different DE input and different delay schedules [18].

Attar et al. [19] adopted reciprocated deposition and improved the geometry of DSS during the CMTGMAW-AM process. The fabricated walls had high geometrical stability [19]. Qi et al. [20] found that the number of layers and passes employed significantly affected the deposition geometry. They suggested that the fabricated geometry was the interplay of ILT, *TS*, and deposition path. It was recommended that the width of

overlapping layers should be less than the width of a single layer to achieve geometric accuracy [20]. Queguineur et al. [21] optimized IPT, *TS*, and *WFS* using DoE. When the macrostructure was correlated with process parameters, it was found that the *WFS* affected bead thickness more, while higher *TS* decreased bead thickness [21]. Chen et al. [22] analysed the deposition geometries of ER2209 and ER2594 filler wires. Upon fabrication, it was observed that the walls had waviness along the deposition and build directions. This variation was more pronounced in the ER2594 sample, indicating the increased geometric sensitivity with the increase in alloy composition.

3.1.2 α-γ Phase Formation

The superior characteristics of DSS alloys are a result of their α-γ phase balance, resulting in a microstructure with two types (duplex) of grains. However, the complex thermal cycles involved in the GMAW-AM process deteriorate the in-built phase balance [23]. This section reflects on findings reported in each of the studies considered involving process parameter optimisation and its effect on the post-fabrication phase ratio.

Hejripour et al. [24] analysed the effect of slow solidification possible by parameter optimisation. Slower cooling resulted in more γ formation and significantly reduced the α phase. Thermal cycles were analysed using both simulation and experimental methods. α and γ phase contents varied along the structure, with the lowest α and highest γ phase contents detected in the middle layers [24]. The study by Knezović et al. [9] also revealed that the α content was minimum in the samples fabricated with higher ILTs. According to Hosseini et al. [18], maintaining a low ILT (150 °C) and a low DE of 0.5 kJ/mm during the CMTGMAW-AM process helped obtain the desired α-γ phase fractions in DSS parts. High ILT (250 °C) and high DE (0.8 kJ/mm) produced excess γ. The findings suggested that the DE input optimisation by a judicious selection of the number of layers and passes employed could help obtain the desired α-γ phase ratio [18].

According to Nagasai et al. [25], the DSS cylinder fabricated using the GMAW-AM process was characterised by anisotropic α and γ phase distribution, resulting in a variable phase ratio across the built direction. Similarly, Kumar and Maji [13] focused on finding suitable process parameters for improving phase uniformity throughout the deposited structure. They reported that the excess γ formation is guaranteed due to the complex nature of the fabrication process. However, the parts had satisfactory mechanical properties [13]. Similarly, Bi et al. [30] employed the CMTGMAW-AM process to develop DSS parts. Heterogeneous distribution of α and γ phases was obtained along the build direction. The α and γ phase ratio reflected an inverse relationship. The bottom section was dominated by the α phase, while the top section contained the highest γ content. Therefore, the microstructure lacked consistency from top to bottom of the deposited structure [30].

While some studies achieved desirable α-γ phase percentages, as shown in Fig. 1, various studies have reported a predominant γ phase formation which compromised the α-γ phase balance and isotropy of formation, as shown in Fig. . Karunanithi et al. [26] also reported an excessively austenitic microstructure. The γ phase content varied between 73% and 85%, while the α phase remained only between 15% to 27%. The low α phase was reported to be due to slow solidification and longer retention of layers in the γ formation range [26]. Microstructural observation done by Eriksson et al. [28] showed that the α phase content was quite low, between 15% to 27%, throughout the SDSS structure deposited by the GMAW-AM process. The microstructure largely possessed SA, WA, and IGA phases due to a higher percentage of Ni and N in the filler wire [28]. According to Kannan et al. [29], the presence of lower α phase and excessive γ phase in SDSS parts resulted in anisotropic hardness and tensile strength properties. The results agreed with previous works on the development of SDSS parts using the GMAW-AM process, involving analysis of geometrical features, α-γ phase ratios, and non-uniform behaviour of mechanical properties [29]. Kemény et al. [27] suggested that the α-γ phase formation and distribution are functions of welding parameters, especially weld voltage. In this study, the relationship between V and phase contents was analysed. It was concluded that the increase in *V* caused an increase in the γ phase [27].

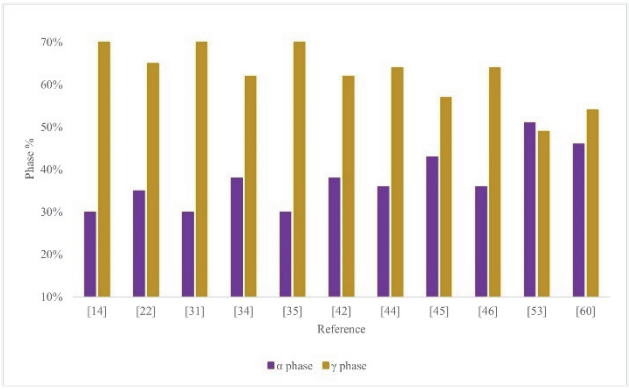

Figure 1 Studies reporting suitable α-γ phase balance

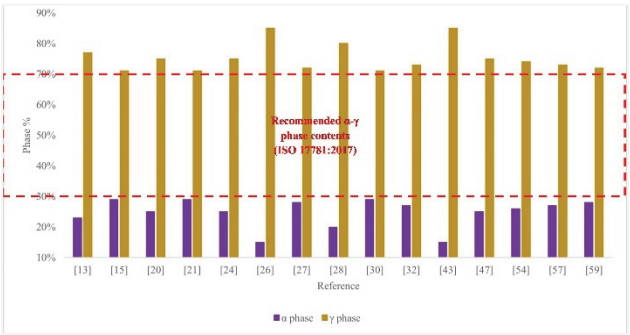

Figure 2 Studies reporting excessive γ formation and depleted α phase

Queguineur et al. [21] analysed the phase formation characteristics of parts deposited with ER2209 and ER2205 filler wires. The α phase percentage with ER2205 was satisfactorily between 48.5% and 52.66%. With the ER2209 filler wire, it was low (28.9%-30.55%). The α phase was drastically reduced with increased DE. The phases were heterogeneously distributed. However, the role of additional N and Ni in the ER2209 filler wire for phase formation remained unexplored [21]. According to Du et al. [31], the α to γ transformation occurred between the temperature range of 1020 °C and 1390 °C. It was stated that the solid-state transformation is nearly absent below

the temperature of 1020 °C at higher cooling rates. The α phase fraction was measured to be 30%, thus signifying the need for parametric optimisation for higher α formation [31].

In another microstructural analysis by Queguineur et al. [33], it was suggested that with low DE input, a higher α phase percentage than the γ phase could be obtained. Contrastingly, the wall sample fabricated using higher DE input had a higher γ phase content than the α phase [33].

Wu et al. (2024) employed variable polarisation (VP) CMTGMAW-AM for fabricating DSS walls [32]. This fabrication method was successful in obtaining a nearly balanced α-γ phase ratio. VP reversed the charge carried by the filler wire and the base plate, optimising the DE input and overcoming the excessive γ formation.

Wittig et al. [34] optimised two parameters, *WFS* and *TS*, and found that the optimization influenced the α and γ phases of both DSS and SDSS parts. The periodic heating and solidification promoted the growth of secondary γ phase particles. Longer times at elevated temperatures resulted in an unacceptable phase balance [34].

Likewise, Liu et al. [36] employed the CMTGMAW-AM process for 3D printing of SDSS walls and conducted microstructural analysis [36]. They observed that the top layer possessed WA, IGA, and SA. However, this was not consistent with the middle and bottom sections, resulting in a heterogeneous phase distribution. The α phase percentages were 29.7%, 33.53%, and 45.80% in the bottom, middle, and top sections, respectively [36].

3.1.3 σ Phase Formation

During the GMAW-AM process, the bottom layers are comparatively less prone to heat entrapment due to the base plate, which acts like a heat sink. Similarly, layers in the top section dissipate heat easily as they are not subjected to subsequent layer deposition. The middle section layers experience protracted heat retention, which often results in the precipitation of deleterious σ phase. They are formed when Fe, Cr, and Mo are no longer soluble in the α matrix, resulting in the precipitation of their tetrahedral intermetallic crystals. Formed between 925 °C and 815 °C temperature range, they degrade toughness, corrosion resistance, and induce embrittlement [37-39].

Recently, Bellamkonda et al. [40] observed the σ phase along the grain boundaries in the DSS cylinder fabricated by the GMAW-AM process. Comparatively, a similar component developed by the CMTGMAW-AM process had no σ phase formation [40]. Wu et al. [41] analysed that suitable ILT and low DE during the GMAW-AM process were instrumental in producing SDSS parts in which no σ phase formation was observed. Prathivraj and Oyyaravelu [42] maintained a constant IPT of 150 °C during the GMAW-AM process to fabricate SDSS 2507 parts. Their results indicated that the IPT maintained during deposition was optimum to help attain a suitable α-γ phase balance without forming the harmful σ phase [42]. According to Eriksson et al. [28], maintaining the DE input during the GMAW-AM process at a low value was vital to contain the formation of detrimental σ phase in the SDSS microstructure [28]. This was experimentally validated by Hosseini et al. [18] by the application of the CMTGMAW-AM process for the fabrication of DSS parts. It was found that higher ILTs achieved during the fabrication process are conducive to σ phase formation [18]. Similarly, Bi et al. [30] showed that lower DE input in the CMTGMAW-AM process prevents σ phase formation in the DSS microstructure. Low DE input was achieved by the optimisation of deposition path, ILT, and *TS* [30].

While the CMTGMAW-AM process can reduce the likelihood of σ phase formation, if the layers remain at temperatures critical for the formation of σ phase for a protracted period, then σ phase formation can occur in both DSS and SDSS components, regardless of the process [34]. In addition to the optimisation of DE, the chemical composition of feed materials, if optimised, can also reduce the chances of σ phase formation. Lervåg et al. [43] found that a higher Ni-containing SDSS wire combined with a lower IPT resulted in no σ phase formation for DE inputs between 0.40 kJ/mm and 0.87 kJ/mm during the CMTGMAW-AM process. This range of DE input was suitable for fabricating components with the required mechanical properties. However, outside this range, repeated thermal cycles caused the formation of detrimental σ phases [43].

3.1.4 Parts Performance

Huang et al. [35] observed that periodic thermal cycles experienced by layers during the process resulted in a built structure characterised by a highly unbalanced α-γ phase ratio. Pant et al. [17] suggested that each of the γ phase morphologies showed unique behaviour, which resulted in a heterogeneous microstructure and anisotropic properties [17]. The non-uniform heat dissipation pattern of the deposited structure and consequent thermal gradients result in heterogeneous grain formation. The resulting microstructure is a mix of grains, including coarsened and fine, epitaxial and equiaxed, columnar and lamellar formations. This is translated into anisotropy of mechanical properties along different orientations of the deposited structure [17, 25, 26, 31, 35, 47]. In the following paragraphs, tensile, toughness, and hardness properties of parts, with focus on the anisotropic behavior of each property, have been reviewed.

According to Knezović et al. [10], the hardness was lowest at 150 °C ILT, indicating an inverse relationship between ILT and hardness property. This was also the trend in the study by Akselsen et al. [12]. Furthering the analysis on ILT, Sales et al. [44] critically analysed its influence on fatigue of DSS parts fabricated by the GMAW-AM process [44]. They observed that low IPTs enhanced the fatigue resistance of components, while no change was observed in their elongation, yield, and tensile strength. Another study by Sales et al. [45] suggested that the placement of beads, *TS*, filler wire diameter, and IPT shape the fatigue life of parts. These parameters were more critical for fatigue than the post-process heat treatment. Recently, Sales et al. [46] suggested that the fatigue life of the longitudinal sample was 50% more than that of the transversal sample. With the optimisation of *TS* and *WFS*, and maintaining 150 °C ILT, the yield strength measured 678 MPa horizontally and 652 MPa vertically, making the anisotropic behaviour of the tensile property evident, though only by 3.98%. It was suggested that the deposition

direction should be perpendicular to the maximum stress direction for improved fatigue life [46].

Karunanithi et al. [26] evaluated the anisotropy of hardness as 19.59 HV0.3, while that of tensile property was up to 20 MPa, between horizontal and vertical samples.

On the other hand, Prathivraj and Oyyaravelu [42] reported uniform hardness and tensile properties. Their results indicated that hardness and load-displacement curves were largely uniform along different directions of the structure. Similarly, Eriksson et al. [28] also found that the SDSS wall samples manufactured using the GMAW-AM process had satisfactory tensile, hardness, and toughness properties. However, at higher DE input, the tensile strength became lower than that of the base plate [28].

Pechetet al. [48] suggested that the optimisation of *TS* and *WFS* improved bead dimensions and tensile strength. No deposition defects, such as inclusions or porosities, were observed.

Bellamkonda et al. [40] compared mechanical characteristics of the DSS cylinders fabricated using the CMTGMAW-AM and conventional GMAW-AM processes. Their results indicated that the parts fabricated using the GMAW-AM process lacked mechanical isotropy, while CMTGMAW-AM-based parts had superior hardness, toughness, and tensile strength [40]. A similar comparison of parts properties was carried out by Posch et al. [15]. The CMTGMAW-AM process had considerably less DE input throughout the fabrication process. The deposited samples had mechanical properties comparable to the values recommended by the product data sheet [15].

Contrarily, according to Pant et al. [17], the DSS components fabricated using the CMTGMAW-AM process did not possess isotropic mechanical properties. Microhardness varied along the top, middle, and bottomsections. While mechanical properties were not isotropic, the parametric optimisation produced the required deposition geometry [17]. Queguineur et al. [33] analysed the microhardness of each of the α-γ phases. They observed that the γ grains had higher hardness than the α grains. However, the microindentation and nanoindentation hardness results were not identical [33].

Bi et al. [30] fabricated a DSS structure using the CMTGMAW-AM process. The anisotropic properties were attributed with the non-uniform α-γ phase distribution. The tensile strength was higher at the bottom, and lower at the top and middle sections [30].

Chen et al. [22] found that the tensile strength of the deposited walls was lower than that of the filler wires. Samples extracted perpendicular to the deposition direction showed the least Young's modulus and tensile strength values. However, the walls exhibited satisfactory ductile properties [22].

Yuan et al. [49] attributed anisotropic hardness and tensile properties to the heterogeneous temperature distribution. Their simulation and experimental results showed that the unidirectional path caused more heat accumulation than the bidirectional deposition, resulting in a large amount of columnar grain formation. This deteriorated the microhardness and tensile properties. However, for either deposition path, the samples had comparable stress distributions.

Figs. 3, Fig. 4, and Fig. 5 show hardness (HV10), microhardness (HV0.1), and tensile characteristics as reported in available studies, respectively.

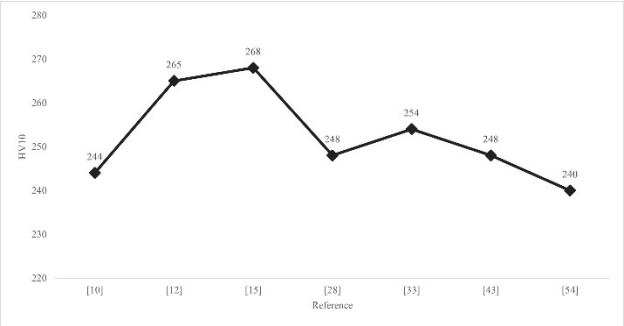

Figure 3 Hardness of DSS parts fabricated by GMAW-AM at 10 kg load

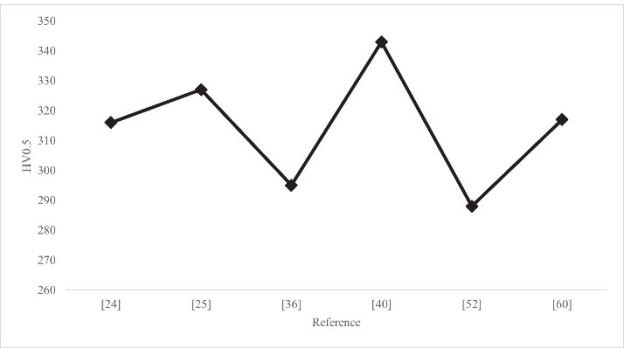

Figure 4 Hardness of DSS parts fabricated by GMAW-AM at 0.5 kg load

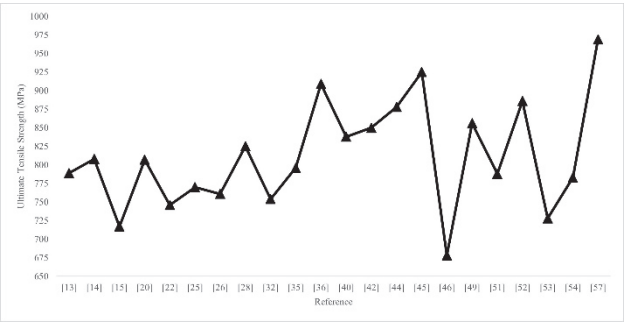

Figure 5 Tensile property of DSS parts fabricated by GMAW-AM

3.2 Shielding Gas Combinations-Based Fabrication

This section focuses on the combination of different gases employed during DSS fabrication by the GMAW-AM process. From quantification analysis, pure Ar gas has most commonly assisted the fabrication process [14, 17-19, 24, 29, 35, 36, 45, 50], followed by Ar and N_2 mixture [32, 33, 51, 52, 69], Ar and O_2 mixture [9, 12, 15, 20-22, 27, 28, 32-34, 43, 44, 46, 48, 53, 54, 64], Ar and NO mixture [12, 28, 43], and Ar and CO_2 mixture [65].

Akbarzadeh et al. [51] analysed the mechanical characteristics obtained under Ar + 2 wt% O_2 and Ar + 2 wt% N_2 combinations. The Ar + 2 wt% N_2 samples had the highest tensile strength. This increase was attributed to the strengthening of γ phase possible with the introduction of N_2 in the fabrication process. The microhardness of the Ar + 2 wt% N_2 sample was higher than that of the Ar and Ar + 2 wt% O_2 samples [51].

Similarly, Wu et al. [53] employed Ar + 2% N_2 and Ar + 2% CO_2 mixtures [53]. The Ar + 2 % N_2 promoted higher and more uniform distribution of the γ phase, compared to the Ar + 2% CO_2 samples, which experienced a lower γ

phase formation. Compared to Ar + 2% CO_2 samples, the Ar + 2% N_2 samples had lower tensile strength anisotropy and higher toughness, which was attributed to their higher γ phase. Also, the Ar + 2% N_2 combination did not imbalance the α-γ phase ratio caused by higher DE input.

Binesh et al. [50] analysed the role of Ar in promoting a suitable α-γ phase balance in DSS parts fabricated by employing the GMAW-AM process. Their 98% Ar + 2% CO_2 combination produced a nearly balanced α-γ phase ratio in the DSS samples. Although the tensile strength was less than that of the wrought counterparts, it was better than that of the samples with only Ar gas [50].

Kemény et al. [27] employed Ar + CO_2 and Ar + He mixtures in combination with 17 V and 19 V weld voltages. They observed that the presence of He in the process decreased the overall α phase content. Their results indicated that the 17 V configuration promoted α formation with Ar + CO_2 mixture due to a lower DE input. However, α content remained low even at 17 V when Ar + He mixture was employed.

Ersan [52] suggested that Ar + O_2 resulted in oxide inclusions. The gas combination also compromised the fatigue resistance and increased vulnerability to crack initiation.

3.3 Special Mechanism and Material-Based Fabrication

Assistance of special mechanisms (also termed in-situ or in-operando mechanisms) and specially designed filler materials can be employed to enhance parts properties [54]. This section includes studies involving chemically modified fabricated parts [54], chemically modified filler wires [57], and employment of double filler wires via innovative process designs [58, 59].

Zhang et al. [54] compared the characteristics of special FC DSS wire and commercial DSS wire. The microstructure analysis indicated an excessive γ phase formation (70%) with commercial wire. The special wires, FCWA-AM-DSS#1 and FCWA-AM-DSS#2, reduced the γ phase to 37% and 45%, respectively.

Later, Zhang et al. [57] specially designed the filler wire to improve the Cr_{Eq} and Ni_{Eq} values of fabricated components. When the Cr_{Eq}:Ni_{Eq} was 2.23, the γ phase content was 45%. It was recommended that the Cr_{Eq}:Ni_{Eq} should be between 1.89 and 2.65 for a desirable phase balance. The fabricated parts exhibited higher tensile strength than their hot-rolled counterparts.

Similarly, Wu et al. [58] modified the chemical composition of fabricated parts by in-situ addition of Ti. This transformed the grain structure from epitaxial columnar to fine equiaxed. Ti additions between 0.5% to 1% (wt%) were recommended [58].

Stützer et al. [59] modified the chemical composition of deposited material by using a supplementary DSS wire with higher Ni content in combination with standard DSS filler wire. The addition of Ni stabilised the α-γ phase balance by optimising the α phase content from 39% to 72% [59].

On the other hand, Yu et al. [60] employed an in-situ trailing-rotation-extrusion mechanism during the CMTGMAW-AM process. By virtue of the contact between the high-speed rotation-extrusion tool and the deposited layers, the layers became plane and flat, and their waviness was overcome. While surface defects such as porosities were still encountered, the samples possessed superior tensile strength and microhardness properties than the as-deposited counterparts [60].

4 DISCUSSION AND ANALYSIS

Analysis of the process optimisation method shows that controlling the DE input is crucial for obtaining parts with suitable microscopic characteristics. The thermal inputis a combined cumulative result of welding parameters (*V*, *I*, and *TS*) and ILTs. Thus, finding the correct set of values for each parameter is vital to producing suitable parts. A higher *V* and *WFS* employed with a lower *TS* might result in a higher deposition rate per unit volume, which might not be appropriate, especially if thin-walled structures are required [13, 17]. Similarly, reducing the *V* and *I* might not ensure sufficient material deposition [14, 21]. Parametric optimisation is not only essential for ensuring geometric precision, but also for the fabricated parts to retain a suitable α-γ phase balance and desirable grain formation characteristics. The correct set of parameters can be systematically determined using tools such as DOE, BOP, OFAT, and MPO [14, 19, 61].

Table 2 A suitable fabrication route for DSS parts fabrication by the GMAW-AM process

Benchmark	Requirement	Recommendations
Microstructure and Mechanical Competency in DSS parts fabricated by the GMAW-AM process	Achieved when the fabricated parts have: 1. Geometric precision, with no porosities, humps, or shrinkages. 2. Suitable α-γ ratio. 3. Uniform grain and boundary characteristics. 4. No σ phases along the grain boundary.	1. Optimised welding parameters and ILT [9, 10, 12, 13, 18, 20, 21]. 2. Optimum cooling conditions to enhance α-γ transformation for achieving a suitable phase balance [10, 18, 21,31-33, 36, 40]. 3. Alloy composition adjustment by suitable shielding gas combination, or special material or mechanism for enhanced mechanical and electrochemical properties [50, 52-54, 57]. 4. Post-process treatment [5, 38].

Similarly, in the case of shielding gas combinations, literature shows that these combinations could be instrumental for achieving desired characteristics in DSS structures deposited by the GMAW-AM process, as long as the combination employed complies with relevant standards [2]. Compared to other gases, N_2 could be vital in promoting a suitable α-γ phase ratio, as it promotes austenisation of otherwise highly ferritic microstructure, especially in parts developed using a smaller number of layers [51, 53].

Special mechanism-assisted fabrication can be handy for overcoming an unbalanced phase ratio. Employment of secondary wire feed in addition to the primary filler wire favorably modified the overall alloy composition of DSS parts and improved their overall metallographic characteristics [57-59]. This method could alter the alloy

composition to improve the overall or a particular mechanical property as dictated by the commercial requirements of fabricated parts. Besides the special mechanisms already employed and researched, future studies should explore additional mechanisms to assist the deposition process, for example, in-situ ultrasonic vibration assistance, pressure application, cold deformation, interpass rolling, etc., to achieve a tailored deposition geometry, grain growth, boundary formation, and α-γ distribution characteristics [63, 66].

The review analysis is summarised in the form of a suitable fabrication route for DSS parts by the GMAW-AM process, as both the cause and cure lie in the fabrication method employed, (Tab. 2).

5 CONCLUSION

In this study, 3 approaches used for DSS parts fabrication by the GMAW-AM were systematically reviewed to develop a suitable fabrication route for DSS parts by the GMAW-AM process. In this regard, relevant studies were reviewed and analysed to draw the following conclusions:

Optimisation of DE is required to improve the energy conservation footprint of the GMAW-AM process. It is highly desirable to devise optimum methods for DSS parts fabrication at the expense of minimum material and energy consumption. While existing studies on process optimisation are commendable, there is plenty of room for more innovative means, for example, ML-based parameter optimisation.

The ILTs and their role in the overall thermal input and solidification mechanism during deposition of DSS parts by the GMAW-AM process need more research attention. Whether the ILT employed during the fabrication process could be any random number, or a specific value with a particular impact on geometrical, microstructural, and mechanical characteristics of fabricated components, and how the dwell (idle) time and time-at-temperature in a certain range constrain the selection of a particular ILT, needs a more definite research answer.

The special mechanisms to assist the fabrication process should be designed and devised so as to overcome the defects otherwise present in the as-deposited parts. Possible examples include in-situ peening, rolling, vibrations, and even alloy composition modifications possible with additional feed wires.

To overcome challenges such as porosity, phase control, and anisotropy of part properties, future studies should expand knowledge about the phase transformation during the fabrication process, the role of N_2 shielding gas and IPT on DSS performance, the effect of solidification conditions on α-γ formation and grain structure, by employing strategies such as real-time thermal control.

The anisotropy of fabricated parts is largely due to heterogeneous phase formation and distribution patterns. If this is an intrinsic microstructure phenomenon, then there is a dire need to analyse phase-wise mechanical characteristics of fabricated components. Knowledge of the characteristic behavior of each phase morphology will enable tailoring the process conditions to the formation of desired phases and their morphologies to finally achieve the required mechanical characteristics.

Acknowledgement

This research was supported by an Australian Government Research Training Program (RTP) Scholarship.

This research paper was funded by the University of Slavonski Brod through the institutional research project Smartmod4IND45, financed by the European Union - NextGenerationEU. The views and opinions expressed in this paper are those of the author and do not necessarily reflect the official position of the European Union or the European Commission. Neither the European Union nor the European Commission can be held responsible for them.

6 REFERENCES

[1] Kahar, S. D. (2017). Duplex stainless steels-an overview. *International Journal of Engineering Research and Application*, *7*(4 Pt 4), 27-36. https://doi.org/10.9790/9622-0704042736

[2] ISO/ASTM 52938-1:2025; Additive Manufacturing of Metals-Environment, Health and Safety. International Organization for Standardization: Geneva, Switzerland, 2025.

[3] Gibson, I., Rosen, D., Stucker, B., Khorasani, M., Rosen, D., Stucker, B., & Khorasani, M. (2021). *Additive manufacturing technologies*, *17*, 160-186. https://doi.org/10.1007/978-3-030-56127-7

[4] Wu, B., Pan, Z., Ding, D., Cuiuri, D., Li, H., Xu, J., & Norrish, J. (2018). A review of the wire arc additive manufacturing of metals: properties, defects and quality improvement. *Journal of manufacturing processes*, *35*, 127-139. https://doi.org/10.1016/j.jmapro.2018.08.001

[5] Zhang, L., Liu, L., Liu, F., Sun, J., & Wang, D. (2024). Effect of Post-Heat Treatment on the Mechanical Properties and Corrosion Behavior of Duplex Stainless Steel fabricated by Wire Arc Additive Manufacturing. *Archives of Metallurgy and Materials*, 667-674. https://doi.org/10.24425/amm.2024.149796

[6] Jafari, D., Vaneker, T. H., & Gibson, I. (2021). Wire and arc additive manufacturing: Opportunities and challenges to control the quality and accuracy of manufactured parts. *Materials & Design*, *202*, 109471. https://doi.org/10.1016/j.matdes.2021.109471

[7] Shi, J., Li, F., Chen, S., Zhao, Y., & Tian, H. (2019). Effect of in-process active cooling on forming quality and efficiency of tandem GMAW-based additive manufacturing. *The International Journal of Advanced Manufacturing Technology*, *101*(5), 1349-1356. https://doi.org/10.1007/s00170-018-2927-4

[8] Li, F., Chen, S., Shi, J., Zhao, Y., & Tian, H. (2018). Thermoelectric cooling-aided bead geometry regulation in wire and arc-based additive manufacturing of thin-walled structures. *Applied Sciences*, *8*(2), 207. https://doi.org/10.3390/app8020207

[9] Knezović, N., Topić, A., Garašić, I., & Jurić, I. (2019). Application of Wire and Arc Additive Manufacturing for Fabrication of Duplex StainlessSteel Product. *Annals of DAAAM& Proceedings*, *30*. https://doi.org/10.2507/30th.daaam.proceedings.081

[10] Knezović, N., Garašić, I., &Jurić, I. (2020). Influence of the interlayer temperature on structure and properties of wire and arc additive manufactured duplex stainless steel product. *Materials*, *13*(24), 5795. https://doi.org/10.3390/ma13245795

[11] Kannan, A. R., Shanmugam, N. S., Rajkumar, V., & Vishnukumar, M. (2020). Insight into the microstructural features and corrosion properties of wire arc additive

manufactured super duplex stainless steel (ER2594). *Materials Letters*, *270*, 127680. https://doi.org/10.1016/j.matlet.2020.127680

[12] Akselsen, O. M., Bjørge, R., Ånes, H. W., Ren, X., & Nyhus, B. (2021). Effect of sigma phase in wire arc additive manufacturing of superduplex stainless steel. *Metals*, *11*(12), 2045. https://doi.org/10.3390/met11122045

[13] Kumar, P. & Maji, K. (2024). Experimental investigations and parametric effects on depositions of super duplex stainless steel in wire arc additive manufacturing. *Proceedings of the Institution of Mechanical Engineers, Part E: Journal of Process Mechanical Engineering*, *238*(4), 1600-1612. https://doi.org/10.1177/09544089231158253

[14] Kumar, P., Mondal, S., & Maji, K. (2024). Analysis and Optimization of Super Duplex Stainless Steel Deposition in Wire Arc Additive Manufacturing Using Machine Learning Techniques. *SAE International Journal of Materials and Manufacturing*, *18*(05-18-01-0008). https://doi.org/10.4271/05-18-01-0008

[15] Posch, G., Chladil, K., & Chladil, H. (2017). Material properties of CMT-metal additive manufactured duplex stainless steel blade-like geometries. *Welding in the World*, *61*(5), 873-882. https://doi.org/10.1007/s40194-017-0474-5

[16] Nikam, P. P., Arun, D., Ramkumar, K. D., & Sivashanmugam, N. (2020). Microstructure characterization and tensile properties of CMT-based wire plus arc additive manufactured ER2594. *Materials Characterization*, *169*, 110671. https://doi.org/10.1016/j.matchar.2020.110671

[17] Pant, S., Kumar, S., & Shahi, A. S. (2024). Microstructural characterization of super duplex stainless steel fabricated using WAAM technique. *Materials Today: Proceedings*, *113*, 230-234. https://doi.org/10.1016/j.matpr.2023.08.331

[18] A Hosseini, V., Högström, M., Hurtig, K., Valiente Bermejo, M. A., Stridh, L. E., & Karlsson, L. (2019). Wire-arc additive manufacturing of a duplex stainless steel: thermal cycle analysis and microstructure characterization. *Welding in the World*, *63*(4), 975-987. https://doi.org/10.1007/s40194-019-00735-y

[19] Attar, H. Z., Fellowes, J. W., Roy, M. J., Hosseini, V. A., & Engelberg, D. L. (2024). Optimizing the phase distribution in arc-based direct energy deposition of duplex stainless steel. *Metallurgical and Materials Transactions A*, *55*(5), 1600-1625. https://doi.org/10.1007/s11661-024-07355-2

[20] Qi, K., Li, R., Hu, Z., Bi, X., Li, T., Yue, H., & Zhang, B. (2022). Forming appearance analysis of 2205 duplex stainless steel fabricated by cold metal transfer (CMT) based wire and arc additive manufacture (WAAM) process. *Journal of Materials Engineering and Performance*, *31*(6), 4631-4641. https://doi.org/10.1007/s11665-022-06587-w

[21] Queguineur, A., Asadi, R., Ostolaza, M., Valente, E. H., Nadimpalli, V. K., Mohanty, G., Hascoët J.-Y., & Ituarte, I. F. (2023). Wire arc additive manufacturing of thin and thick walls made of duplex stainless steel. *The International Journal of Advanced Manufacturing Technology*, *127*(1), 381-400. https://doi.org/10.1007/s00170-023-11560-5

[22] Chen, M. T., Chen, Y., Zuo, W., Yun, X., Zhao, O., Liu, S. W., & Xu, F. (2024). Experimental investigation on the tensile behavior of wire arc additively manufactured duplex stainless steel plates. *Engineering Structures*, *321*, 118764. https://doi.org/10.1016/j.engstruct.2024.118764

[23] Pellegrino, J. V. (2014). *Duplex Stainless Steel: Atlas of Microstructures*. Materials Technology Institute, Incorporated.

[24] Hejripour, F., Binesh, F., Hebel, M., & Aidun, D. K. (2019). Thermal modeling and characterization of wire arc additive manufactured duplex stainless steel. *Journal of Materials Processing Technology*, *272*, 58-71. https://doi.org/10.1016/j.jmatprotec.2019.05.003

[25] Nagasai, B. P., Dwivedy, M., Malarvizhi, S., Balasubramanian, V., Ramaswamy, A., Snehalatha, P., & Vegesna, N. (2024). Study on properties and microstructure of wire arc additive manufactured 2209 duplex stainless steel. *Metallography, Microstructure, and Analysis*, *13*(3), 519-531. https://doi.org/10.1007/s13632-024-01089-8

[26] Karunanithi, S. P., Arasappan, R. K., & Nallathambi, S. S. (2024). Microstructural evolution, mechanical and electrochemical performance of Duplex stainless steel fabricated by wire arc additive manufacturing with ER2209 filler wire. *Steel research international*, *95*(12), 2400425. https://doi.org/10.1002/srin.202400425

[27] Kemény, D. M., Sándor, B., Varbai, B., & Katula, L. T. (2023). The effects of arc voltage and shielding gas type on the microstructure of wire arc additively manufactured 2209 duplex stainless steel. *Advances in Materials Science*, *23*(4), 62-82. https://doi.org/10.2478/adms-2023-0023

[28] Eriksson, M. C. F., Lervåg, M., Sørensen, C., Robertstad, A., Brønstad, B. M., Nyhus, B., Aune, R., Ren, X., & Akselsen, O. M. (2018). Additive manufacture of superduplex stainless steel using WAAM. *MATEC Web of Conferences 188*, *03014*(2018). https://doi.org/10.1051/matecconf/201818803014

[29] Kannan, A. R., Shanmugam, N. S., Ramkumar, K. D., & Rajkumar, V. (2021). Studies on super duplex stainless steel manufactured by wire arc additive manufacturing. *Transactions of the Indian Institute of Metals*, *74*(7), 1673-1681. https://doi.org/10.1007/s12666-021-02257-y

[30] Bi, X., Li, R., Hu, Z., Gu, J., & Jiao, C. (2022). Microstructure and texture of 2205 duplex stainless steel additive parts fabricated by the cold metal transfer (CMT) wire and arc additive manufacturing (WAAM). *Metals*, *12*(10), 1655. https://doi.org/10.3390/met12101655

[31] Du, C., Ren, X., Pan, Q., & Li, Y. (2022). Preferential orientation and mechanical properties anisotropy of wire and arc additive manufactured duplex stainless steel. *Materials Characterization*, *194*, 112277. https://doi.org/10.1016/j.matchar.2022.112277

[32] Wu, K., Shen, C., Xin, J., Ding, Y., Wang, L., Zhou, W., Ruan, G., Zhang, Y., Li, F., Reddy, K. M., Chen, M.-T., & Hua, X. (2024). Tailoring the microstructure and tensile properties of directed energy deposition-arc buildup 2209 duplex stainless steel by variable polarity energy arrangement. *Journal of Manufacturing Processes*, *127*, 433-445. https://doi.org/10.1016/j.jmapro.2024.08.018

[33] Queguineur, A., Cherukuri, R., Lambai, A., Dalal, M. S., Peura, P., Mohanty, G., Hascoët J.-Y. &Ituarte, I. F. (2024). Correlated high throughput nanoindentation mapping and microstructural characterization of wire and arc additively manufactured 2205 duplex stainless steel. *Welding in the World*, *68*(9), 2247-2257. https://doi.org/10.1007/s40194-024-01795-5

[34] Wittig, B., Zinke, M., & Jüttner, S. (2021). Influence of arc energy and filler metal composition on the microstructure in wire arc additive manufacturing of duplex stainless steels. *Welding in the World*, *65*(1), 47-56. https://doi.org/10.1007/s40194-020-00995-z

[35] Huang, X., Kwok, C. T., Niu, B., Luo, J., Zou, X., Cao, Y., Yi, L., Pan, L., Qiu, W., & Zhang, X. (2023). Anisotropic behavior of super duplex stainless steel fabricated by wire arc additive manufacturing. *Journal of Materials Research and Technology*, *27*, 1651-1664. https://doi.org/10.1016/j.jmrt.2023.10.005

[36] Liu, A., Yin, B., Zhang, D., & Wen, P. (2023). Microstructure, mechanical and electrochemical properties of wire-arc additively manufactured duplex stainless steel. *Science and Technology of Welding and Joining*, *28*(4), 268-276. https://doi.org/10.1080/13621718.2022.2151766

[37] Song, S., Li, G., Wu, B., Cai, Q., & He, X. (2024). Effect of Mn content on the microstructure and corrosion resistance of duplex stainless steels fabricated by wire arc additive manufacturing. *Metals and Materials International*, 1-16. https://doi.org/10.1007/s12540-024-01842-2

[38] Sanjeeviprakash, K., Sankarapandian, S., Rajesh Kannan, A., & Shanmugam, N. S. (2025). Influence of heat treatment on the microstructure and thermal conductivity of duplex stainless steel manufactured via wire arc additive manufacturing. *Proceedings of the Institution of Mechanical Engineers, Part E: Journal of Process Mechanical Engineering*, 09544089241309449. https://doi.org/10.1177/09544089241309449

[39] Llorca-Isern, N., López-Luque, H., López-Jiménez, I., & Biezma, M. V. (2016). Identification of sigma and chi phases in duplex stainless steels. *Materials Characterization*, *112*, 20-29. https://doi.org/10.1016/j.matchar.2015.12.004

[40] Bellamkonda, P. N., Dwivedy, M., Sudersanan, M., & Visvalingam, B. (2025). Influence of welding processes on the microstructure and mechanical properties of duplex stainless steel parts fabricated by wire arc additive manufacturing. *Metals and Materials International*, *31*(2), 368-391. https://doi.org/10.1007/s12540-024-01753-2

[41] Wu, S., Guo, C., Liu, W., Ying, M., & Li, Y. (2023). Wire arc additive manufacturing using ER2594 duplex stainless steel. *Transactions of the Indian Institute of Metals*, *76*(1), 249-258. https://doi.org/10.1007/s12666-022-02746-8

[42] Prathivraj, S. & Oyyaravelu, R. (2024). Effect of interpass temperature on austenite ferrite ratio of wire arc additive manufactured 2507 Super Duplex Stainless Steel. *Materials Letters*, *361*, 136125. https://doi.org/10.1016/j.matlet.2024.136125

[43] Lervåg, M., Sørensen, C., Robertstad, A., Brønstad, B. M., Nyhus, B., Eriksson, M., Aune, R., Ren, X., Akselsen, O. M., & Bunaziv, I. (2020). Additive manufacturing with superduplex stainless steel wire by cmt process. *Metals*, *10*(2), 272. https://doi.org/10.3390/met10020272

[44] Sales, A., Kotousov, A., Perilli, E., & Yin, L. (2022). Improvement of the fatigue resistance of super duplex stainless-steel (SDSS) components fabricated by wire arc additive manufacturing (WAAM). *Metals*, *12*(9), 1548. https://doi.org/10.3390/met12091548

[45] Sales, A., Kotousov, A., & Yin, L. (2021). Design against fatigue of super duplex stainless steel structures fabricated by wire arc additive manufacturing process. *Metals*, *11*(12), 1965. https://doi.org/10.3390/met11121965

[46] Sales, A., Khanna, A., Hughes, J., Yin, L., & Kotousov, A. (2024). Fatigue crack growth rates and crack tip opening loads in CT specimens made of SDSS and manufactured using WAAM. *Materials*, *17*(8), 1842. https://doi.org/10.3390/ma17081842

[47] Bercelli, L., Caër, C., Dhondt, M., Doudard, C., Beaudet, J., & Calloch, S. (2024). Full-field measurements of the microstructure's effect on the mechanical behaviour of a wire and arc additively manufactured duplex stainless steel. *Materials & Design*, *244*, 113223. https://doi.org/10.1016/j.matdes.2024.113223

[48] Pechet, G., Hascoet, J. Y., Rauch, M., Ruckert, G., & Thorr, A. S. (2020). Manufacturing of a hollow propeller blade with WAAM process-from the material characterisation to the achievement. *Industry 4.0 - Shaping the Future of the Digital World*, 155-160. https://doi.org/10.1201/9780367823085-28

[49] Yuan, Y., Li, R., Bi, X., Gu, J., & Jiao, C. (2022). Experimental and numerical investigation of CMT wire and arc additive manufacturing of 2205 duplex stainless steel. *Coatings*, *12*(12), 1971. https://doi.org/10.3390/coatings12121971

[50] Binesh, F., Bahrami, A., Hebel, M., & Aidun, D. K. (2021). Preservation of natural phase balance in multi-pass and wire arc additive manufacturing-made duplex stainless steel structures. *Journal of Materials Engineering and Performance*, *30*(4), 2552-2565. https://doi.org/10.1007/s11665-021-05593-8

[51] Akbarzadeh, E., Yurtışık, K., HakanGür, C. E. M. İ. L., Saeid, T., & Tavangar, R. (2024). Influence of shielding gas on the microstructure and mechanical properties of duplex stainless steel in wire arc additive manufacturing. *Metals and Materials International*, *30*(7), 1977-1996. https://doi.org/10.1007/s12540-023-01623-3

[52] Ersan, R. B. (2023). *Fracture Toughness of Wire Arc Additive Manufactured Duplex Stainless Steel Grade 2509.* Master's thesis, Middle East Technical University, Turkey.

[53] Wu, K., Shen, C., Xu, P., Xin, J., Ding, Y., Wang, L., Zhou, W., Ruan, G., Zhang, Y., Li, F., Chen, M.-T., & Hua, X. (2024). Revealing the evolution of microstructure and mechanical properties with deposition energy and shielding gas to achieve phase-balanced directed energy deposition of 2205 duplex stainless steel. *Materials Science and Engineering: A*, *915*, 147197. https://doi.org/10.1016/j.msea.2024.147197

[54] Zhang, Y., Cheng, F., & Wu, S. (2021). The microstructure and mechanical properties of duplex stainless steel components fabricated via flux-cored wire arc-additive manufacturing. *Journal of Manufacturing Processes*, *69*, 204-214. https://doi.org/10.1016/j.jmapro.2021.07.045

[55] Hosseini, V. A. & Karlsson, L. (2019). Physical and kinetic simulation of nitrogen loss in high temperature heat affected zone of duplex stainless steels. *Materialia*, *6*, 100325. https://doi.org/10.1016/j.mtla.2019.100325

[56] Sun, T., Tan, W., Chen, L., & Rollett, A. (2020). In situ/operando synchrotron x-ray studies of metal additive manufacturing. *MRS Bulletin*, *45*(11), 927-933. https://doi.org/10.1557/mrs.2020.275

[57] Zhang, Y., Wu, S., & Cheng, F. (2022). A specially-designed super duplex stainless steel with balanced ferrite: austenite ratio fabricated via flux-cored wire arc additive manufacturing: Microstructure evolution, mechanical properties and corrosion resistance. *Materials Science and Engineering: A*, *854*, 143809. https://doi.org/10.1016/j.msea.2022.143809

[58] Wu, S., Zhang, Y., Xue, M., & Cheng, F. (2024). Grain refinement of flux-cored wire arc additively manufactured duplex stainless steel through in-situ alloying of Ti. *Materials Characterization*, *209*, 113749. https://doi.org/10.1016/j.matchar.2024.113749

[59] Stützer, J., Totzauer, T., Wittig, B., Zinke, M., & Jüttner, S. (2019). GMAW cold wire technology for adjusting the ferrite-austenite ratio of wire and arc additive manufactured duplex stainless steel components. *Metals*, *9*(5), 564. https://doi.org/10.3390/met9050564

[60] Yu, C., Zhao, Y., Xu, W., Dong, C., Guo, C., Deng, J., Li, Z., & Miao, S. (2022). Trailing rotating-extrusion-assisted wire arc additive manufacturing of duplex stainless steel. *Science and Technology of Welding and Joining*, *27*(8), 629-637. https://doi.org/10.1080/13621718.2022.2105993

[61] Meena, R. P., Yuvaraj, N., & Vipin (2024). Optimization of process parameters of cold metal transfer welding-based wire arc additive manufacturing of super Duplex stainless steel using response surface methodology. *Proceedings of the Institution of Mechanical Engineers, Part E: Journal of Process Mechanical Engineering*, 09544089241230878. https://doi.org/10.1177/09544089241230878

[62] Wang, H., Klarić, Š., & Havrlišan, S. (2025). Study of Weld Bead Geometry for GMAW Additive Manufacturing of Duplex Stainless Steel. *FME Transactions*, *53*(3), 471-481. https://doi.org/10.5937/fme2503471W

[63] Uhamir, P., Klarić, Š., & Havrlišan, S. (2025). Preliminary Investigation of Additive Manufacturing of Duplex Stainless Steel Parts with Vibrational Assistance. *Strojarske tehnologije u izradi zavarenih konstrukcija I proizvoda, SBZ 2025.*, 156-166.

[64] Chiniforoush, E. A., Gholizadeh, T., Jandaghi, M. R., Moverare, J., & Gür, C. H. (2025). Impact of active to inert shielding gas transition on the corrosion behavior of wire arc

additively manufactured duplex stainless steel. *Materials & Design*, *253*, 113907. https://doi.org/10.1016/j.matdes.2025.113907

[65] Chiniforoush, E. A., Gholizadeh, T., Jandaghi, M. R., Moverare, J., & Gür, C. H. (2025). Investigation of Travel Speed Effects on Microstructure and Corrosion Behavior of Duplex Stainless Steel in Wire-Based DED Additive Manufacturing. *Journal of Materials Research and Technology*. https://doi.org/10.1016/j.jmrt.2025.06.143

[66] Chiniforoush, E. A., Zargari, H. H., Jandaghi, M. R., Moverare, J., Warsi, R., & Gür, C. H. (2025). A sustainable strategy for wire arc additive manufacturing of high-performance duplex stainless Steel: Microstructural refinement and mechanical anisotropy reduction. *Materials Science and Engineering: A*, *943*, 148785. https://doi.org/10.1016/j.msea.2025.148785

Nomenclature

3D	Three-Dimensional
α-γ	Ferrite-Austenite
σ	Sigma
Al	Aluminium
BOP	Bead-On-Plate
CMT	Cold Metal Transfer
CO_2	Carbon di Oxide
CQI	Continuous Quality Improvement
Cr	Chromium
Cr_{Eq}	Chromium Equivalent
DE	Deposition Energy
DED-Arc	Directed Energy Deposition-Arc
DOE	Design-Of-Experiment
DSS	Duplex Stainless Steel
FC	Flux Cored
Fe	Iron
GMAW-AM	Gas Metal Arc Welding-Additive Manufacturing
He	Helium
I	Weld Current
IGA	Intragranular Austenite
ILT	Interlayer Temperature
IPT	Interpass Temperature
MAM	Metal Additive Manufacturing
MIG-AM	Metal Inert Gas-Additive Manufacturing
ML	Machine Learning
Mo	Molybdenum
MPO	Multi-Parameter Optimisation
N	Nitrogen
Ni	Nickel
Ni_{Eq}	Nickel Equivalent
NO	Nitrogen Oxide
OFAT	One-Factor-A-Time
SA	Secondary Austenite
SDSS	Super Duplex Stainless Steel
SGFR	Shielding Gas Flow Rate
SS	Stainless Steel
Ti	Titanium
TS	Travel Speed
V	Weld Voltage
VP	Variable Polarisation
WA	Widmanstätten Austenite
WAAM	Wire Arc Additive Manufacturing
WFS	Wire Feed Speed

Contact information:

Uhamir PATRICK
(Corresponding author)
Charles Darwin University, Faculty of Science and Technology,
Ellengowan Drive, Casuarina, Northern Territory, Australia
E-mail: uhamir.patrick@students.cdu.edu.au

Stefanija KLARIC, Professor
Charles Darwin University, Faculty of Science and Technology,
Ellengowan Drive, Casuarina, Northern Territory, Australia
E-mail: stefanija.klaric@cdu.edu.au

Sara HAVRLISAN, Assistant Professor
(Corresponding author)
University of Slavonski Brod, Mechanical Engineering Faculty,
Trg I. B. Mazuranic 2, 35000 Slavonski Brod, Croatia
E-mail: shavrlisan@unisb.hr